

ELECTROPLATED COPPER COATINGS ON 304L AND  
316L STAINLESS STEELS FOR MITIGATION OF  
METAL DUSTING CORROSION IN  
METHANE/HYDROGEN ENVIRONMENT

BY

FARG IBRAHEEM MOHAMED HAIDER

A thesis submitted in fulfilment of the requirement for the  
degree of Doctor of Philosophy (Engineering)

Kulliyyah of Engineering  
International Islamic University Malaysia

FEBRUARY 2019

## ABSTRACT

Metal dusting corrosion is high-temperature degradation of metals and alloys into dust-like fine particles. It is often encountered in petrochemical industry, where metals and alloys extensively exposed to carbon-containing gases at high temperature. It is a costly issue in the industry; millions of dollars have been invested annually in the fields of monitoring, controlling and prevention of metal dusting corrosion to avoid potential dangers in the environments. Metal dusting initiates as a result of unwanted carbon formation on the surface of metallic engineering installations. At high temperature, solid carbon diffuses into the metal/alloy matrix to form a carburised layer on the surface. Under certain conditions, this carburised region may become unstable and decompose into carbon and metal/alloy particles, as well as other corrosion products. Such as metal particles may further catalyse the carbon deposition and the process are hence accelerated. Thus, the primary aim of this study is to prevent carbon diffusion into metal in order to mitigate the metal dusting corrosion by using an electroplating copper coating on 304L and 316L stainless steels. Therefore, coated and uncoated 304L and 316L samples were exposed to metal dusting environment in a 10% to 50 % CH<sub>4</sub>/H<sub>2</sub> gas mixture, at temperature range of 600 °C to 800 °C, and a pressure of 1 atm, leading to carbon activities from 0.203 to 3.289 for 100 hours. Optical microscopy (OM) results revealed that the electroplating copper coating mitigates carbon from diffuse into metal, so no carburization zone was formed, compared with non-coated samples which displayed clear carburization were formed for both 304L and 316L stainless steel at temperatures more than 600 °C and gas mixture 20 % CH<sub>4</sub>/H<sub>2</sub> and above where carbon activity approach to 1. Weight gain test showed non-significant weight gain on coated samples compared to uncoated samples. These values of weight gain increase with increase the temperature or/and CH<sub>4</sub>/H<sub>2</sub> gas mixture. These results were also confirmed by X-Ray Diffraction (XRD) and scanning electron microscope (SEM) coupled with energy dispersive x-ray (EDX) which showed no carbides formed on the surfaces of coated samples. M<sub>7</sub>C<sub>3</sub> carbides were formed on the surface of uncoated samples as a result of carbon diffusion in the metal and react with elements. In these experiments, electroplated copper samples showed negligible carbon deposition on the surface and no carbon diffusion into the metal. Thus, copper electroplating coating is solution to mitigate metal dusting corrosion

## خلاصة البحث

تآكل الغبار المعدني ينتج عنه تحلل المعادن والسبائك الى جزيئات دقيقة تشبه الغبار عند درجات الحرارة العالية. وغالبا ما يواجه هذا النوع من التآكل في صناعة البتروكيماويات ، حيث تتعرض المعادن والسبائك الى نطاق واسع من الغازات المحتوية على الكربون عند درجة حرارة عالية. وهذه العملية مكلفة في الصناعة ؛ فقد استثمرت ملايين الدولارات سنوياً في مجالات مراقبة وضبط ومنع تآكل الغبار المعدني لتجنب المخاطر المحتملة كالانفجرات و - أو انبعاث الغازات السامة تحت ظروف الضغط والحرارة المرتفعة. يبدأ الغبار المعدني نتيجة ترسب الكربون غير المرغوب فيه على سطح المنشآت الهندسية المعدنية. عند درجة حرارة عالية ، ينتشر الكربون الصلب داخل مصفوفة المعدن / سبيكة لتشكيل طبقة كربنة على السطح. في ظل ظروف معينة ، قد تصبح هذه المنطقة الكربونية غير مستقرة وتحلل الى جزيئات الكربون والمعادن وسبائك التآكل الأخرى. بعض الجسيمات المعدنية قد تزيد من تحفيز ترسيب الكربون مما يترتب عليه تسريع العملية. وبالتالي ، فإن الهدف الأساسي من هذه الدراسة هو منع انتشار الكربون إلى داخل المعدن من أجل التخفيف من حدة التآكل الغباري المعدني باستخدام طلاء نحاسي مطلي بالكهرباء على 304L و 316L الفولاذ المقاوم للصدأ. لذلك ، عرضت عينات 304L و 316L المطلية وغير المطلية لبينة الغبار المعدني في خليط من غاز  $CH_4 / H_2$  بنسب من 10% الى 50%، وفي نطاق درجة حرارة 600 درجة مئوية الى 800 درجة مئوية ، وضغط 1 ضغط جوي ، وكن نشاط الكربون  $a_c$  يتراوح من 0.203 إلى 3.289 لمدة 100 ساعة. أظهرت نتائج الفحص الميكروسكوبي (OM) أن طلاء النحاس الكهربائي يخفف من الانتشار الكربوني إلى المعدن ، لذلك لم يتم تشكيل أي منطقة كربنة ، مقارنة بالعينات غير المغلفة التي عرضت كربنة واضحة تم تشكيلها لكلا من الفولاذ 304L و 316L في درجات حرارة أكثر من  $600^{\circ}C$  ونسبة مزيج الغاز 20%. وما فوق  $CH_4 / H_2$  حيث يصل النشاط الكربون  $a_c$  إلى 1. أظهر اختبار اكتساب الوزن عدم وجود وزن على العينات المطلية مقارنة مع العينات غير المطلية. تزداد قيم زيادة الوزن مع زيادة درجة الحرارة أو - و نسبة خليط الغاز  $CH_4 / H_2$  هذه النتيجة أكدت أيضا عن طريق حيود الأشعة السينية (XRD) والمجهر الإلكتروني الماسح (SEM) إلى جانب الأشعة السينية المشتتة للطاقة (EDX) التي أظهرت عدم وجود كربيد على أسطح العينات المطلية. تم تشكيل كربيد  $M_7C_3$  على سطح العينات غير المطلية نتيجة للكربون المنتشر داخل المعدن وتفاعله مع العناصر. في هذه التجارب ، أظهرت العينات المطلية بالنحاس بطريقة الكلاء الكهربائي ترسب لا يذكر للكربون على السطح مما أدى لعدم وجود انتشار للكربون داخل المعدن. وبالتالي ، فإن طلاء النحاس الكهربائي هو حل للتخفيف من تآكل الغبار المعدني

## **APPROVAL PAGE**

The thesis of Farg Ibraheem Mohamed Haider has been approved by the following:

---

Suryanto  
Supervisor

---

Mohd. Hanafi bin Ani  
Co-Supervisor

---

Md. Abdul Maleque  
Internal Examiner

---

Astuty Binti Amrin  
External Examiner

---

Mohd. Amri Bin Lajis  
External Examiner

---

Saim Kaya Dibi  
Chairman

## DECLARATION

I hereby declare that this thesis is the result of my own investigation, except where otherwise stated. I also declare that it has not been previously or concurrently submitted as a whole for any other degrees at IIUM or other institutions.

Farg Ibraheem Mohamed Haider

Signature.....

Date .....

INTERNATIONAL ISLAMIC UNIVERSITY MALAYSIA

**DECLARATION OF COPYRIGHT AND AFFIRMATION OF  
FAIR USE OF UNPUBLISHED RESEARCH**

**ELECTROPLATED COPPER COATINGS ON 304L AND 316L  
STAINLESS STEELS FOR MITIGATION OF METAL DUSTING  
CORROSION IN METHANE/HYDROGEN ENVIRONMENT**

I declare that the copyright holder of this thesis is International Islamic University  
Malaysia.

Copyright © 2019 by Farg Ibraheem Mohamed Haider. All rights reserved.

No part of this unpublished research may be reproduced, stored in a retrieval system, or transmitted, in any form or by any means, electronic, mechanical, photocopying, recording or otherwise without prior written permission of the copyright holder except as provided below.

1. Any material contained in or derived from this unpublished research may be used by others in their writing with due acknowledgement.
2. IIUM or its library will have the right to make and transmit copies (print or electronic) for institutional and academic purposes.
3. The IIUM library will have the right to make, store in a retrieval system and supply copies of this unpublished research if requested by other universities and research libraries.

By signing this form, I acknowledge that I have read and understand the IIUM  
Intellectual Property Right and Commercialization policy.

Affirmed by Farg Ibraheem Mohamed Haider

.....  
Signature

.....  
Date

*This thesis is dedicated to*

*My wife and our children*

*For their love, understanding and company comfort of eyes*

*forever and ever*

## ACKNOWLEDGEMENTS

Foremost, all praises are due to Almighty Allah (SWT) for granting me the wisdom, guidance, knowledge, and strength to complete this thesis.

I wish to express my gratitude and appreciation to my thesis supervisor Assoc. Prof. Dr. Suryanto “main supervisor”, an Assoc. Professor in Kulliyah (Faculty) of Manufacturing and Materials Engineering in International Islamic University Malaysia (IIUM), who has given constant guidance, friendly enthusiasm, constructive criticism, valuable suggestions and encouragement during the pursuit of this research.

Furthermore, I would like to express my heartfelt appreciation to my thesis co-supervisor Assoc. Prof. Dr. Mohd Hanafi bin Ani, an Assoc. Professor in Kulliyah (Faculty) of Manufacturing and Materials Engineering in International Islamic University Malaysia (IIUM), for his scholarly advice and guidance from beginning till the very end of this thesis.

Apart from aforementioned in academic world, deepest gratitude to the technical team of IIUM involving Br. Edhuan (corrosion), Br. Zakaria (tool and die & metrology), Br. Ibrahim (metallography and SEM), Br. Faisal and Br. Zahir (workshop) and Br. Rahimie (surface engineering) and others I could not mention here. Without your help, the work can not be completed. You all are the unsung heroes.

Finally, special thanks to my ever loving and admirable sweet heart Asma and our lovely kids Khairia, Mohamed, Meiral, and Serein for their patient, sacrifice, and support. I pray Allah to grant us long life to enjoy the fruit of the sacrifice.



# TABLE OF CONTENTS

Abstract .....	ii
Abstract in Arabic .....	iii
Approval Page .....	iv
Declaration .....	v
Copyright Page .....	vi
Dedication .....	vii
Acknowledgements .....	viii
List of Tables .....	xii
List of Figures .....	xiv
List of Abbreviations .....	xix
List of Symbols .....	xx
<b>CHAPTER ONE: INTRODUCTION .....</b>	<b>1</b>
1.1 Background of Study .....	1
1.2 Problem Statement .....	3
1.3 Research Philosophy .....	4
1.4 Objectives of the Research .....	4
1.6 Research Scope .....	5
1.7 Thesis Organization .....	6
<b>CHAPTER TWO: LITERATURE REVIEW .....</b>	<b>7</b>
2.1 Metal Dusting .....	7
2.2 Caburisation .....	7
2.3 Thermodynamic Considerations .....	8
2.4 Carbon Diffusion .....	11
2.5 Mechanisms of Metal Dusting .....	15
2.5.1 For Low Alloy Steels –Type I .....	16
2.5.2 For Nickel-Based Alloys Steels –TypeII .....	18
2.5.3 For Austenitic Stainless Steels -Type III .....	18
2.6 Control and Prevention of Metal Dusting .....	21
2.6.1 Effect of Process Conditions on Metal Dusting .....	21
2.6.2 Effect of Surface Poisoning on Metal Dusting .....	22
2.6.3 Effect of Alloying Elements on Metal Dusting .....	23
2.6.3.1 Effect of Nickel .....	23
2.6.3.2 Effect of Chromium .....	24
2.6.3.3 Effect of Aluminium And Silicon .....	25
2.6.3.4 Effect of Copper .....	25
2.6.3.5 Effect of Carbide Formers .....	26
2.6.4 Effect of Mechanical and Surface Treatments on Metal Dusting ..	26
2.6.4.1 Surface Treatments .....	27
2.6.4.2 Coatings .....	27
2.7 Electroplating of Copper .....	29
2.7.1 Electroplating Kinetics of Copper Dissolution and Deposition .....	30
2.7.2 Types of Electroplating .....	31
2.7.2.1 Direct Current Electroplating .....	31

2.7.2.2 Pulse Plating .....	32
2.7.3 Applications of Electroplating .....	33
2.8 Experimental Design Plan .....	33
2.8.1 Response Surface Methodology .....	33
2.8.2 Central Composite Design .....	34
2.8.3 Preference of Central Composite Design.....	36

### **CHAPTER THREE: EXPERIMENTAL DESIGN AND METHODOLOGY 37**

3.1 Introduction .....	37
3.2 Materials .....	38
3.3 Copper Electroplating on 304L and 316L Stainless Steels .....	40
3.3.1 Sample Preparation .....	40
3.3.2 Copper Electroplating .....	40
3.4 Measurement of Coating Thickness .....	41
3.5 Optimization of Coating Parameters. ....	42
3.4.1 Parametric Study and the Response of Design Plan .....	42
3.4.2 Design Plan Matrix.....	43
3.6 Exposure of Samples to Metal Dusting Environment .....	44
3.6.1 Experimental Apparatus.....	44
3.6.2 Experimental Procedure.....	46
3.6.3 Experimental Conditions .....	47
3.6.3.1 Parametric Study and the Response of Design Plan.....	47
3.6.3.2 Design Plan Matrix.....	48
3.7 Characterization Techniques .....	49
3.7.1 Optical Microscopy.....	49
3.7.2 Scanning Electron Microscope (SEM) with Energy Dispersive X-Ray (EDX) .....	50
3.7.3 Adhesion Testing .....	50
3.7.4 X-Ray Diffraction (XRD) .....	51

### **CHAPTER FOUR: RESULTS AND DISSCUSSION.....52**

4.1 Introduction .....	52
4.2 Copper Electroplating on 304L and 316L Stainless Steels.....	52
4.2.1 Morphology of Copper Electroplating.....	53
4.2.2 Phase of Copper Electroplating.....	53
4.2.3 Adhesive Strength of Copper Electroplating .....	54
4.3 Adhesion of Copper Electroplating .....	55
4.3.1 Morphology of Copper Electroplating.....	55
4.3.2 Scratch Ridges of Copper Electroplating .....	56
4.3.3 Influence of Electroplating Parameters on Adhesive Strength.....	57
4.3.3.1 Model for Adhesive Strength .....	60
4.3.3.2 Model Adequacy Test.....	65
4.3.4 Model Graph for Adhesive Strength.....	70
4.3.5 Optimization of Adhesive Strength Performance .....	76
4.3.6 Confirmation Experiments.....	77
4.3.7 Summary .....	79
4.4 Thickness of Copper Electroplating .....	79
4.4.1 Morphology of Copper Electroplating.....	79
4.4.2 Influence of Electroplating Time on Coating Thickness .....	80

4.4.3 Summary .....	82
4.5 Metal Dusting on 304L and 316L Stainless Steels.....	83
4.5.1 Weight Gain .....	83
4.5.1.1 Effect of Metal Dusting Parameters on Weight Gain.....	85
4.5.1.2 Fit Summary Statistics.....	86
4.5.1.3 Analysis of Variance (ANOVA) .....	88
4.5.1.4 Model Analysis for Weight Gain .....	89
4.5.1.5 Model Adequacy Test.....	90
4.5.1.6 Summary of Statistics Model .....	90
4.5.1.7 Regression Model Diagnostic Test.....	91
4.5.1.8 Surface and Contour Plots for weight gain.....	93
4.5.2 Carbon Diffusion in 304L and 316L Stainless Steels.....	95
4.5.3 Effect of Gas Cocentrations (CH <sub>4</sub> /H <sub>2</sub> ) On 304L and 316L Stainless Steels.....	96
4.5.3.1 Cross-Sectional Morphology.....	96
4.5.3.2 Phase Identification .....	97
4.5.3.3 Surface Morphology .....	99
4.5.4 Effect of Temperature on 304L And 316L Stainless Steels.....	102
4.5.4.1 Cross-sectional Morphology .....	102
4.5.4.2 Phase Identification .....	103
4.5.4.3 Surface Morphology .....	105
4.5.5 Summary .....	107
4.6 Metal Dusting on Coated 304Land 316L Stainless Steels.....	109
4.6.1 Weight Gain .....	109
4.6.2 Effect of Gas Concentration (CH <sub>4</sub> /H <sub>2</sub> ) on Coated 304L and 316L Stainless Steels .....	110
4.6.2.1 Cross-Sectional Morphology.....	110
4.6.2.2 Phase Identification .....	111
4.6.2.3 Surface Morphology .....	113
4.6.3 Effect of Temperature on Coated 304L and 316L Stainless steels	115
4.6.3.1 Cross-Sectional Morphology.....	115
4.6.3.2 Phase Identification .....	116
4.6.3.3 Surface Morphology .....	117
4.6.4 Effect Copper Coating Thickness Against Metal Dusting.....	120
4.6.4.1 Cross-Sectional Morphology.....	120
4.6.4.2 Phase Identification .....	121
4.6.4.3 Surface Morphology .....	123
4.6.5 Summary .....	123

**CHAPTER FIVE: CONCLUSION AND RECOMMENDATION.....126**

5.1 Conclusion .....	126
5.2 Contribution to Knowledge .....	128
5.3 Recommendation for Further Studies.....	129

**REFERENCES.....131**

## LIST OF TABLES

Table 2.1	Interaction parameters of alloying elements on the activity coefficients for carbon in austenitic steel at 900°C	13
Table 2.2	Tabulation of error function values (erf)	15
Table 3.1	Chemical composition in weight percent (wt%) of 304L and 316L SS	38
Table 3.2	The electroplating parameters used for copper deposition	40
Table 3.3	Factors and levels in CCD experimental design plan of electroplating	42
Table 3.4	Design matrix and response for electroplating copper coating	43
Table 3.5	Factors and levels in CCD experimental design plan of metal dusting	48
Table 3.6	Central composite design (CCD) matrix and response weight gain	49
Table 4.1	Central composite design (CCD) matrix and response adhesive strength	59
Table 4.2	Fit summary of adhesive strength (non-transforms)	61
Table 4.3	Fit summary of adhesive strength (square root transforms)	62
Table 4.4	Analysis of variance for square root of adhesive strength (complete model terms)	63
Table 4.5	Analysis of variance for square root of adhesive strength (improved model terms)	63
Table 4.6	Summary of model statistics for adhesive strength	66
Table 4.7	Optimization condition for process parameter response	76
Table 4.8	Optimal solution generated in the response	77
Table 4.9	Analysis of confirmation tests for electroplating process parameters	77
Table 4.10	Analysis of confirmation report for adhesive strength	78

Table 4.11	Thickness measured by weight gain and cross-sectional methods	80
Table 4.12	Central composite design (CCD) matrix and response weight gain	86
Table 4.13	Fit summary for weight gain (non-transforms)	87
Table 4.14	Fit summary for weight gain (square root transforms)	88
Table 4.15	Analysis of variance for square root of weight gain (complete model terms)	88
Table 4.16	Summary of model statistics for weight gain	91
Table 4.17	Weight gain for uncoated and coated 304L and 316L stainless steels	110

## LIST OF FIGURES

Figure 1.1	Metal dusting corrosion	1
Figure 2.1	Equilibrium constants for reactions which may produce carbon in metal dusting environments	10
Figure 2.2	Concentration profiles for nonsteady-state diffusion taken at three different times, $t_1$ , $t_2$ , and $t_3$ .	14
Figure 2.3	Schematic of the proposed mechanism of metal dusting on iron and low alloy steels	17
Figure 2.4	Schematic illustration of the metal dusting mechanism on high alloyed steels and CrFeNi-alloys	20
Figure 2.5	Scheme of a copper electroplating unit	31
Figure 2.6	Central composite design in (a) two and (b) three dimensions	35
Figure 3.1	Flow chart of the research work	39
Figure 3.2	Schematic showing the experimental setup	45
Figure 3.3	Temperature-time cycle	45
Figure 3.4	Temperature-time profile for temperature calibration at 700°C	46
Figure 3.5	Temperature-distance profile for hot zone calibration at 700°C	47
Figure 4.1	OM image and SEM micrograph of Cu-coated at 150 g/L CuSO <sub>4</sub> , 150 g/L H <sub>2</sub> SO <sub>4</sub> and 60 mA/cm <sup>2</sup>	53
Figure 4.2	X-ray diffraction patterns (XRD) of electroplating copper coating on 304L and 316L stainless steels	54
Figure 4.3	OM images for the scratch ridges of Cu-coated on 304L and 316L stainless steels at 150g/L CuSO <sub>4</sub> , 150g/L H <sub>2</sub> SO <sub>4</sub> and 60 mA/cm <sup>2</sup>	54
Figure 4.4	SEM micrographs of the copper electroplating according to Table 3.4 (a) Std. 6, (b) Std 10, (c) Std 2, (d) Std 11, (e) Std 13 and (f) Std 14	56

Figure 4.5	OM images for scratch ridges of the Cu-coatings according to Table 3.4 (a) Std. 6, (b) Std 10, (c) Std 2, (d) Std 11	57
Figure 4.6	Box-Cox plot for power transforms of adhesive strength	61
Figure 4.7	Perturbation plot for adhesive strength	65
Figure 4.8	Normal probability of residual adhesive strength.	68
Figure 4.9	Plot of residuals versus predicted values for adhesive strength.	69
Figure 4.10	Plot of residuals against run order for adhesive strength	70
Figure 4.11	3D surface and contour plots of adhesive strength with $\text{CuSO}_4$ and $\text{H}_2\text{SO}_4$ concentration (a) surface plot and (b) contour map	73
Figure 4.12	3D surface and contour plots of adhesive strength with $\text{CuSO}_4$ concentration and current density (a) surface plot and (b) contour map	74
Figure 4.13	3D surface and contour plots of adhesive strength with $\text{H}_2\text{SO}_4$ concentration and current density (a) surface plot and (b) contour map	75
Figure 4.14	Percentage error % for confirmation test runs	78
Figure 4.15	Optical microscopy image of cross section Cu-coating on 304L and 316L stainless steels substrates	79
Figure 4.16	The error percentage between the two methods	81
Figure 4.17	Coating thickness as a function of the time	82
Figure 4.18	Weight gain vs temperature at different gas concentrations.	84
Figure 4.19	Weight gain vs $\text{CH}_4/\text{H}_2$ concentration at different temperatures	85
Figure 4.20	Box-Cox plot for power transforms of weight gain	87
Figure 4.21	Perturbation plot for weight gain	90
Figure 4.22	Normal probability of residual for weight gain	92
Figure 4.23	Plot of residuals versus predicted values for weight gain	92
Figure 4.24	Plot of residuals against run order for weight gain	93

Figure 4.25	3D surface and contour plots of weight gain with Temperature and CH <sub>4</sub> concentration (a) surface plot and (b) contour map	94
Figure 4.26	The carbon concentration vs distance from the surface	95
Figure 4.27	Cross-sectional images of OM of 304L samples a) As received, b) 750 °C in 20% CH <sub>4</sub> /H <sub>2</sub> and c) 750 °C in 40% CH <sub>4</sub> /H <sub>2</sub>	96
Figure 4.28	Cross-sectional images of OM of 316L samples a) As received, b) 750 °C in 20% CH <sub>4</sub> /H <sub>2</sub> and c) 750 °C in 40% CH <sub>4</sub> /H <sub>2</sub>	96
Figure 4.29	X-ray diffraction patterns (XRD) of 304L as received and exposed to different gas concentration	98
Figure 4.30	X-ray diffraction patterns (XRD) of 316L as received and exposed to different gas concentration	98
Figure 4.31	SEM-EDX spectra for 304L (a) as received (b) 750 °C in 20% CH <sub>4</sub> /H <sub>2</sub> (c) 750 °C in 40% CH <sub>4</sub> /H <sub>2</sub>	100
Figure 4.32	SEM-EDX spectra for 316L (a) as received (b) 750 °C in 20% CH <sub>4</sub> /H <sub>2</sub> (c) 750 °C in 40% CH <sub>4</sub> /H <sub>2</sub>	101
Figure 4.33	Cross-sectional images of OM of 304L samples a) As received, b) 650 °C in 20% CH <sub>4</sub> /H <sub>2</sub> and c) 750 °C in 20% CH <sub>4</sub> /H <sub>2</sub>	102
Figure 4.34	Cross-sectional images of OM of 316L samples a) As received, b) 650 °C in 20% CH <sub>4</sub> /H <sub>2</sub> and c) 750 °C in 20% CH <sub>4</sub> /H <sub>2</sub>	102
Figure 4.35	X-ray diffraction patterns (XRD) of 304L as received and exposed to different temperatures	103
Figure 4.36	X-ray diffraction patterns (XRD) of 316L as received and exposed to different temperatures	104
Figure 4.37	SEM-EDX spectra for 304L (a) as received (b) 650 °C in 20% CH <sub>4</sub> /H <sub>2</sub> (c) 750 °C in 20% CH <sub>4</sub> /H <sub>2</sub>	106
Figure 4.38	SEM-EDX spectra for 316L (a) as received (b) 650 °C in 20% CH <sub>4</sub> /H <sub>2</sub> (c) 750 °C in 20% CH <sub>4</sub> /H <sub>2</sub>	108
Figure 4.39	Cross-sectional images of OM of Cu-coated 304L samples with 80 μm coating thickness, at a) 750 °C in 20% CH <sub>4</sub> /H <sub>2</sub> and b) 750 °C in 40% CH <sub>4</sub> /H <sub>2</sub>	111



Figure 4.40	Cross-sectional images of OM of Cu-coated 316L samples with 80 $\mu\text{m}$ coating thickness, at a) 750 $^{\circ}\text{C}$ in 20% $\text{CH}_4/\text{H}_2$ and b) 750 $^{\circ}\text{C}$ in 40% $\text{CH}_4/\text{H}_2$	111
Figure 4.41	X-ray diffraction patterns (XRD) of Cu-coated 304L with 80 $\mu\text{m}$ untreated and exposed to different gas concentration	112
Figure 4.42	X-ray diffraction patterns (XRD) of Cu-coated 316L with 80 $\mu\text{m}$ untreated and exposed to different gas concentration	112
Figure 4.43	SEM-EDX spectra for 80 $\mu\text{m}$ coated 304L (a) Cu-coated untreated (b) 750 $^{\circ}\text{C}$ in 20 % $\text{CH}_4/\text{H}_2$ (c) 750 $^{\circ}\text{C}$ in 40% $\text{CH}_4/\text{H}_2$	113
Figure 4.44	SEM-EDX spectra for 80 $\mu\text{m}$ coated 316L (a) Cu-coated untreated (b) 750 $^{\circ}\text{C}$ in 20 % $\text{CH}_4/\text{H}_2$ (c) 750 $^{\circ}\text{C}$ in 40% $\text{CH}_4/\text{H}_2$	114
Figure 4.45	Cross-sectional images of OM of 80 $\mu\text{m}$ coated 304L samples at a) 650 $^{\circ}\text{C}$ in 20 % $\text{CH}_4/\text{H}_2$ and b) 750 $^{\circ}\text{C}$ in 20 % $\text{CH}_4/\text{H}_2$	115
Figure 4.46	Cross-sectional images of OM of 80 $\mu\text{m}$ coated 316L samples at a) 650 $^{\circ}\text{C}$ in 20 % $\text{CH}_4/\text{H}_2$ and b) 750 $^{\circ}\text{C}$ in 20 % $\text{CH}_4/\text{H}_2$	115
Figure 4.47	X-ray diffraction patterns (XRD) of Cu-coated 304L untreated and exposed to different temperature	116
Figure 4.48	X-ray diffraction patterns (XRD) of Cu-coated 316L untreated and exposed to different temperature	117
Figure 4.49	SEM-EDX spectra for 80 $\mu\text{m}$ coated 304L (a) Cu-coated untreated (b) 650 $^{\circ}\text{C}$ in 20 % $\text{CH}_4/\text{H}_2$ (c) 750 $^{\circ}\text{C}$ in 20 % $\text{CH}_4/\text{H}_2$	118
Figure 4.50	SEM-EDX spectra for 80 $\mu\text{m}$ coated 316L (a) Cu-coated untreated (b) 650 $^{\circ}\text{C}$ in 20 % $\text{CH}_4/\text{H}_2$ (c) 750 $^{\circ}\text{C}$ in 20 % $\text{CH}_4/\text{H}_2$	119
Figure 4.51	Cross-sectional images of OM of coated 304L samples at 750 $^{\circ}\text{C}$ in 20 % $\text{CH}_4/\text{H}_2$ at coating thickness a) 40 $\mu\text{m}$ and b) 80 $\mu\text{m}$	120
Figure 4.52	Cross-sectional images of OM of coated 316L samples at 750 $^{\circ}\text{C}$ in 20 % $\text{CH}_4/\text{H}_2$ at coating thickness a) 40 $\mu\text{m}$ and b) 80 $\mu\text{m}$	120
Figure 4.53	X-ray diffraction patterns (XRD) of Cu-coated 304L with different coating thickness	121

Figure 4.54	X-ray diffraction patterns (XRD) of Cu-coated 316L with different coating thickness	122
Figure 4.55	SEM-EDX spectra for coated 304L (a) untreated (b) 750 °C in 40 % CH <sub>4</sub> /H <sub>2</sub> with 40μm (c) 750 °C in 40 % CH <sub>4</sub> /H <sub>2</sub> with 80μm	124
Figure 4.56	SEM-EDX spectra for coated 316L (a) untreated (b) 750 °C in 40 % CH <sub>4</sub> /H <sub>2</sub> with 40μm (c) 750 °C in 40 % CH <sub>4</sub> /H <sub>2</sub> with 80μm	125

## LIST OF ABBREVIATIONS

BCC	Body centered cubic
CCD	Central composite design
CVD	Chemical vapour deposition
DOE	Design of experiment
EDM	Electrical discharge machining
EDX	Energy dispersive x-ray
FCC	Face centered cubic
MD	Metal dusting
mm	Millimetre
OM	Optical microscopy
PVD	Physical vapour deposition
RSM	Response surface methodology
SEM	Scanning electron microscopy

## LIST OF SYMBOLS

$P_{H_2}$	Partial pressure of hydrogen
$P_{CH_4}$	Partial pressure of methane
$\Delta G$	Gibbs energy
$\Delta H$	Change in the enthalpy
$\mu m$	Micrometre
$a_c$	Carbon activity
Ar	Argon
C	Carbon
CH <sub>4</sub>	Methane
CO	Carbon monoxide
Cr	Chromium
Cr <sub>7</sub> C <sub>3</sub>	Chromium carbide
Cu	Copper
CuSO <sub>4</sub>	Copper sulphate
Fe	Iron
Fe <sub>7</sub> C <sub>3</sub>	Iron carbide
H <sub>2</sub>	Hydrogen
H <sub>2</sub> SO <sub>4</sub>	Sulfuric acid
Mn	Manganese
Mo	Molybdenum
N	Nitrogen
Ni	Nickel
P	Phosphorus
S	Sulfur
Si	Silicon

# CHAPTER ONE

## INTRODUCTION

### 1.1 BACKGROUND OF STUDY

Metal dusting (MD) can be defined as a high temperature phenomenon leading to the disintegration of materials, such as iron, nickel, and cobalt-based alloys, into powder (or dust) as shown in Figure 1.1. The powder is generally composed of metal, metal carbide, carbon and oxide particles. MD can alternatively be described as a catastrophic carburisation that occurs in environments with high carbon activities (i.e. more than unity) and low oxygen partial pressures (Gunawardana et al. (2013); Put et al., 2015; Slabbert, 2013). Carburisation plays a key role in the metal dusting process and unstable carbides are apparently a major factor in the reaction (Slabbert, 2012).

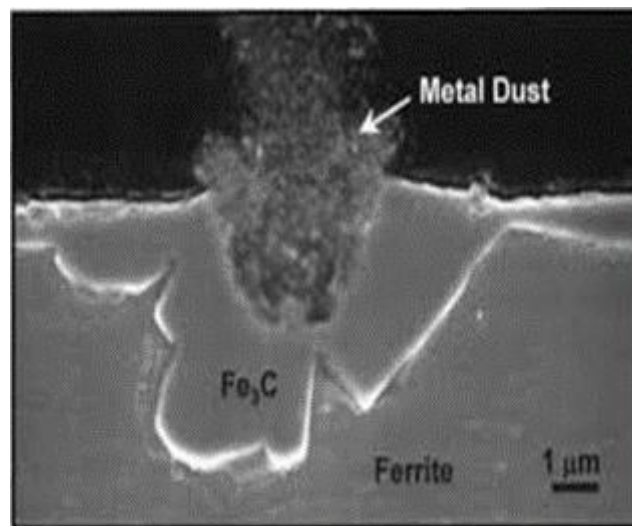


Figure 1.1: Metal dusting corrosion (Chun et al., 2002)

Metal dusting usually occurs at elevated temperatures within the range of 400-800 °C (Grabke (2003); Young et al., 2011). However, the temperature range has not

been well identified as it has also been reported to be 450-800 °C (Grabke, 1995; Voisey et al., 2006a) or 450-900 °C (Agarwal et al., 2001). On the contrary, in heat-treating industry, metal dusting has been reported to have at times occurred in the temperature range of 900-930 °C (Al-Meshari & Little, 2009). In addition, it is documented that metal dusting has happened at temperature as high as 1100 °C in strongly reducing environments (Hrivnak et al., 2005). Theoretically, metal dusting is possible at any temperature if the carbon activity is greater than one (Grabke, 1998).

Metal dusting is an old problem that is responsible for many early failures in a wide variety of industrial sectors. It has been encountered in carbon monoxide (CO) (Mishakov et al., 2013), methane (CH<sub>4</sub>) and mixture of methane and hydrogen (CH<sub>4</sub>/H<sub>2</sub>) (Grabke et al., 2002; Liu et al., 2016a), ethane (C<sub>2</sub>H<sub>6</sub>) (Grabke, 1999), propane (C<sub>3</sub>H<sub>8</sub>) (Ackermann et al., 2005), and butane (C<sub>4</sub>H<sub>10</sub>) (Mishakov et al., 2013), and other mixtures of similar gases. Therefore, MD is most commonly encountered in steam reforming processes such as the production of hydrogen or syngas for ammonia and methanol applications. At elevated temperatures, CO and hydrocarbons tend to dissociate on metal surfaces and form carbon. The carbon is then transferred to the solid phase, draws the susceptible metals out of their homogeneous solid matrix, which leads to pitting, general attack, and finally to the breakdown of the materials (Grabke & Schütze, 2014b).

Controlling and mitigate MD corrosion needs to be taken into consideration since it poses issues to production units. The main method to eliminate the influence of MD on petrochemical industrial equipment currently is replacing the corroded section, and detailed monitoring and periodic inspection are required as well. While, these add large extra costs. For example, the US Department of Energy has reported that annually

220-290 million dollars is spent to replace unit due to metal dusting corrosion in hydrogen production industry (Ma, 2017)

## **1.2 PROBLEM STATEMENT**

Metal dusting poses a great threat to the petrochemical industries such as steam reforming processes, production of hydrogen or syngas of ammonia. Metal dusting causes not only failures or degradation of components but also heavy economic loss. Extensive research efforts have been devoted to the mitigation of failures. Despite the efforts, these problems still remain troublesome and likely to continue to pose threat to the concerned industries. Therefore, there is a strong drive to operate deeper into the metal dusting region in order to create more energy efficient processes. So, there is a significant interest in protecting metal parts from metal dusting. The key to suppressing metal dusting is to stop the dissociation of the carbon source or subsequent carbon diffusion into the susceptible materials.

There are several methods to protect metal from MD, which have been discussed in the literature review including modifying the process conditions, surface poisoning, alloying, chemical, mechanical and laser treatments as well as coatings. Each method has advantages and disadvantages. Changes of process conditions are not an option due to the process requirements in most cases and the use of poisonous chemicals is still limited due to its interference with downstream processes. Newly developed alloys are sometimes not sufficiently resistant and expensive due to the large quantities involved. Mechanical and chemical surface treatments are not always applicable, and the lifetime of coatings is often limited by adhesion problems.

To tackle these challenges, surface coating of the austenitic stainless steel has been attempted by several researchers using the physical vapour deposition (PVD) and chemical vapour deposition (CVD) techniques. Despite these efforts, these techniques are expensive, complicated and difficult to recoating at the site because they operate at very high temperatures and vacuums also it requires a cooling water system to dissipate large heat loads. To overcome these previous issues, this research will be investigated how to use a copper coating on 314L, 316L by Electrodeposition technique against MD corrosion.

### **1.3 RESEARCH PHILOSOPHY**

Significant efforts have been made on coating of austenitic stainless steel against MD corrosion. However, coating lifetime still the major problem of coating application. Moreover, repair/reapply coating on site is difficult and its cost is very expensive. Since Cu is non catalytic to carbon reaction with a metallic surface (Alstrup et al., 1998; Bernardo et al., 1985; Zhang et al., 2007), therefore, using copper coating by electroplating might improve the lifetime of the coating by repair/reapply coating on the site. Also, this technique is inexpensive and simple to use which may attract the chemical and petrochemical industries to use this technique to protect the stainless-steel structures and save them without catastrophic failure.

### **1.4 OBJECTIVES OF THE RESEARCH**

The primary aim of this work is to study the electroplated copper coatings on 304L and 316L stainless steels for mitigation of metal dusting corrosion in CH<sub>4</sub>/H<sub>2</sub> environment.

The objectives are: